

Skeletal myoblast implants induce minor propagation delays, but do not promote arrhythmias in the normal swine heart

Javier Moreno^{1*}†, Jorge G. Quintanilla^{1†}, Antonio López-Farré¹, Tamara Archondo¹, Raquel Cervigón², Paloma Aragoncillo¹, Elena Usandizaga¹, Jacobo Silva¹, Cruz Rodríguez-Bobada¹, José Luis Rojo³, Nicasio Pérez-Castellano¹, Sergey Mironov⁴, Lluís Mont⁵, Teresa Pérez de Prada¹, Carlos Macaya¹ and Julián Pérez-Villacastín¹

¹Optical Mapping Laboratory, Arrhythmia Unit and Cardiovascular Institute, Hospital Clínico San Carlos, Madrid, Spain; ²Group of Bioengineering Innovation, University of Castilla-La Mancha, Cuenca, Spain; ³Signal Theory Department, Rey Juan Carlos University, Madrid, Spain; ⁴Center for Arrhythmia Research, University of Michigan, Ann Arbor, MI, USA; and ⁵Arrhythmia Unit, Hospital Clínic, Barcelona, Spain

Received 20 April 2010; accepted after revision 1 July 2010; online publish-ahead-of-print 30 July 2010

Aims

Whether skeletal myoblast (SM) implants are proarrhythmic is still controversial due to conflicting pre-clinical and clinical data. We hypothesized that if SM implants are arrhythmogenic, they will facilitate the induction of ventricular tachyarrhythmias by promoting heterogeneous propagation of activation wavefronts.

Methods

Skeletal myoblast cells were harvested from 10 pigs. A month later, $125 \pm 37 \times 10^6$ cells were subepicardially injected in an area of $\sim 2 \text{ cm}^2$ at the anterolateral aspect of the left ventricle. Four weeks later, a ventricular stimulation protocol was conducted. Once explanted, epicardial wavefronts over SM and adjacent control areas were optically mapped. Eight saline-injected animals were used as controls. To compare with clear arrhythmogenic substrates, propagation patterns were also evaluated in infarcted hearts and on a SM-implanted heart following amiodarone infusion.

Results

In SM hearts, fibrosis and differentiated SM cells were consistently found and no tachyarrhythmias were induced. Wavefronts propagated homogeneously over SM and adjacent areas, with no late activation zones, as opposed to the infarcted hearts. The time required for the wavefronts to depolarize both areas were similar, becoming only slightly longer at SM areas after an extra-stimulus ($P = 0.025$). Conduction velocities and APD_{90} were also similar. Saline hearts showed similar results. The extent of the conduction delay was not related to the number of injected SM cells.

Conclusion

In normal swine hearts, myoblast implants promote localized fibrosis and slightly retard epicardial wavefront propagation only after extra-stimuli. However, SM implants are not associated with local re-entry and do not facilitate ventricular tachyarrhythmias in the whole normal heart.

Keywords

Optical mapping • Skeletal myoblasts • Arrhythmias

Introduction

Pilot clinical studies on the transplantation of skeletal muscle precursor cells (skeletal myoblasts; SM) into infarcted areas seemed promising.^{1–3} However, sustained ventricular arrhythmias were initially reported,^{1–3} challenging initial high expectations.^{4,5}

However, the suggested proarrhythmia has not been confirmed by recent major clinical trials that have shown that ventricular arrhythmia rates are as to be expected for such a selected sick population^{4–7} so controversy remains.^{8–11}

Animal studies have produced inconclusive data.^{12–16} Thus, to further evaluate the safety of SM implants, we tested in a large

* Corresponding author. Tel/fax: +34 913303527, Email: jmoreno@secardiologia.es

† These authors contributed equally.

Published on behalf of the European Society of Cardiology. All rights reserved. © The Author 2010. For permissions please email: journals.permissions@oxfordjournals.org.

whole mammal heart (swine) if implants *per se* facilitate the induction of ventricular arrhythmias in the normal *in situ* heart and if they can promote theoretically proarrhythmic propagation patterns.

Methods

Experimental model and surgical protocol

This study complied with national guidelines (RD 1201/2005). Female adult Pietrain pigs (30–40 kg) were selected. Ten animals

underwent SM implants. All surgeries were performed under general anaesthesia (propofol, fentanyl, and isoflurane) by a cardiac surgeon involved in clinical trials with SM implants.

A 5–7 gr biopsy of the sternohyoid muscle was retrieved for myoblast isolation. A month later, a left thoracotomy was performed to expose the anterolateral aspect of the left ventricle. Two non-absorbable suture stitches (4–0 polypropylene) were placed as markers (Figure 1A). The SM suspension (1.5–2 mL) was injected tangentially by 3–5 subepicardial injections over a ~ 2 cm² area around a midpoint between the two sutures using a prebent 25 gauge needle. Four weeks later, hearts were

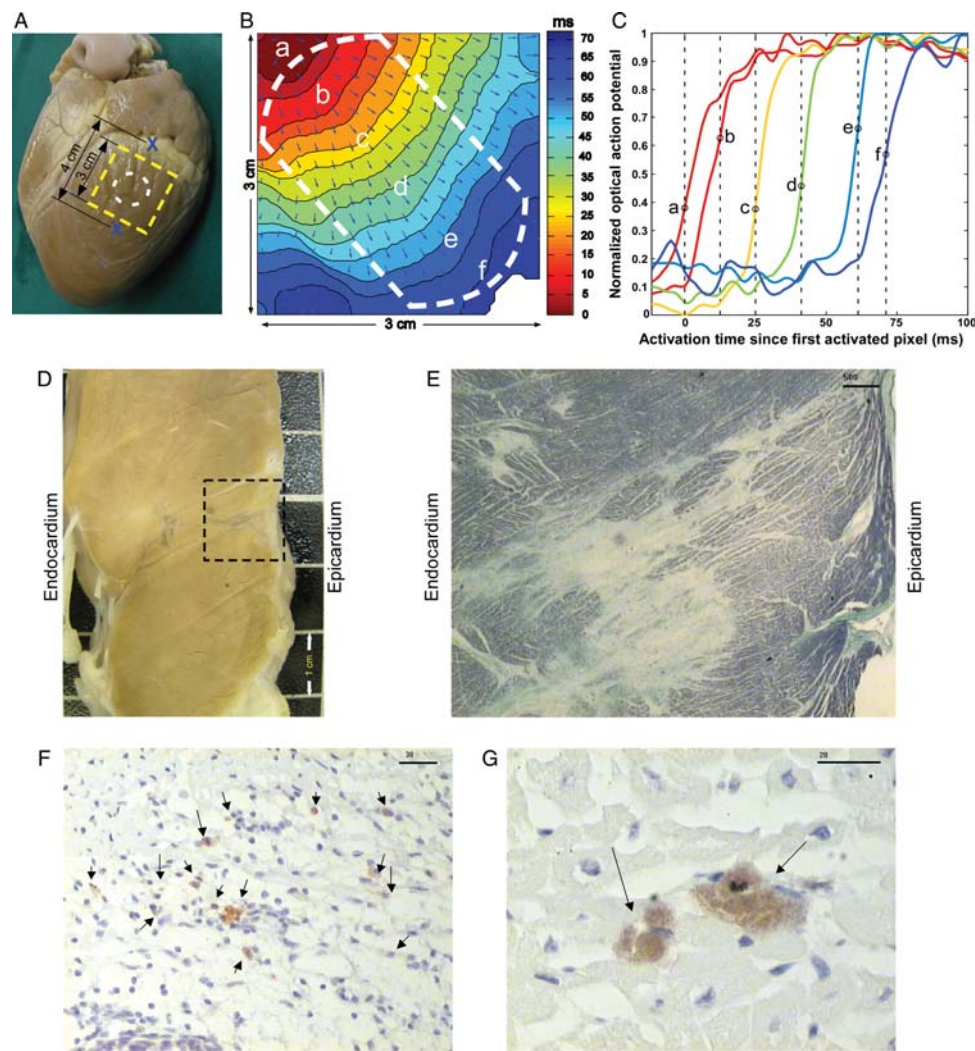


Figure 1 (A) The location of the implant zone and sutured ties (X) used as references. The white circle shows the injection site and the yellow square represents the filmed area. (B) An example of velocity vectors over an isochrone map. The white dashed line marks the area selected to calculate the mean CV. (C) Phase 0 of local action potentials taken at different pixels from the adjacent isochrone map, as used to depict the activation wavefront. The local activation time corresponds to the timing of the maximum positive slope as marked by a small circle. (D) Macroscopic view of an implanted zone showing a whitish triangular wedge embedded in normal myocardium. Linear lesions represent the injection trajectories. The affected zone is limited to ~ 1 cm depth. (E) Masson's stain of an implant zone. White areas representing fibrosis can be observed surrounded by normal myocardium. Scale bar = 500 μ m. (F) Microscopic detection of implanted cells. Arrows point at differentiated myotubes stained with BMDV1025 antibodies dispersed within the fibrous tissue in an implant zone. Scale bar = 30 μ m. (G) At injury boundaries, away from connective tissue, groups of 3–4 cells stained with BMDV1025 (arrows) are shown among normal cardiomyocytes. Scale bar = 20 μ m.

exposed and programmed electrical stimulation (PES) was performed. In one animal, this procedure was undertaken 5 months after SM implant to evaluate a long-term proarrhythmia.

Isolation and preparation of myoblasts

Biopsies were digested with trypsin (0.5 mg/mL) and collagenase (0.5 mg/mL). After filtering through a nylon net (80 μ m), cells were grown in the Ham-F12 medium (GIBCO-BRL) supplemented with 20% fetal calf serum and 1% penicillin/streptomycin (GIBCO-BRL). Cultures were incubated and passages were performed (every \sim 10 days) at subconfluence (80%) to prevent myotube formation. Skeletal myoblast were harvested after 2–4 passages for a total of \sim 100–200 \times 10⁶ cells. Before implant, cells were washed to eliminate any fetal calf serum and re-suspended in the autologous serum (50–80 \times 10⁶ cells/mL). Assessment of myoblasts was performed by flow cytometry using antibodies against CD45 and desmin.

In situ data: programmed electrical stimulation

Any spontaneous arrhythmia, including ventricular ectopies (VE), was monitored (Prucka CardioLab, GE) during a 30 min interval, under anaesthesia, before manipulation of the heart, at the second (pre-SM implant) and the third surgical procedures. At the latter procedure, PES was conducted pacing close to the implant zone. Pacing was performed at 500, 400, and 300 ms basic drive cycle length (BDCL) adding up to two extra-stimuli. We also paced at the most rapid cycle length ensuring 1:1 capture and then suddenly stopped to record any triggered activity. No atrial stimulation was performed as no major atrial proarrhythmia would be expected.

Isolated heart preparation and optical recordings

Hearts were then explanted and taken to a Langendorff's apparatus to be perfused and superfused with 37°C oxygenated Tyrode's solution. Pacing was performed at the left upper corner of the field of view (3 \times 3 cm²) over an SM zone or an adjacent (more septal or lateral) control area. Pacing included 500, 400, and 300 ms (S1) adding one extra-stimulus (S2) to 500 and 400 ms. Optical mapping (OM) movies (2") were recorded by a CCD camera (Dalsa Inc., Ontario, Canada) at 800 frames/s, using Di4ANEPPS.¹⁷ Recordings included S1 and S2 beats 10 ms longer than the effective ventricular refractory period (EVRP). Movies were recorded with a spatial resolution of 64 \times 64 pixels: 0.47 mm/pixel.

To stabilize, the heart was gently compressed against the surface of the superfusion chamber. Recordings of the initial propagation of depolarization wavefronts are usually free from motion artefacts, so electromechanical uncouplers (Cyto-D) were only used in a single experiment as control.

Control hearts and additional experiments

Eight animals underwent the whole protocol but were injected 2 mL of saline instead. Additional experiments were performed

to register overt epicardial slow conduction. Three animals underwent transmural ischaemic infarctions by percutaneous balloon occlusion during 90 min of the mid anterior descending artery in one case and proximal circumflex artery in two. Four weeks later, OM and PES were performed over the borders of the infarcted epicardium on the isolated hearts. Another animal underwent the regular protocol but 1.5 mL of sterile 98% ethanol was injected instead to induce a localized chemical infarction. On one of the SM-injected isolated hearts, after completion of the protocol, stimulation was repeated 5 min after adding 300 mg amiodarone to the 5 L of perfusion.

Data processing and analysis

The propagation dynamics of S1 and S2 depolarization wavefronts were analysed and isochrone maps were computed (Figure 1B and C). We defined total activation time (TAT) as the time required for a wavefront to depolarize the whole field of view. Local velocity vectors were computed.¹⁸ When homogeneous propagation was found, we defined mean conduction velocity (CV) as the average of the values of all vectors in a selected wide area parallel to the direction of the fastest propagation (Figure 1B). APD₉₀ duration was defined as optical action potential duration at 90% re-polarization, averaging values from 10 non-adjacent pixels.

S2 beats propagate slower than S1 beats, so TAT after S2 (TAT-S2) should be longer than after S1 beats. We wanted to quantify whether TAT-S2 were longer at SM zones, compared with adjacent ones, and if the potential delay in TAT-S2 over SM zones was related to the number of injected cells. Thus, we calculated for each SM-implanted heart (at 500 and 400 ms) the per cent variation in TAT-S2 over the SM zone referred to the adjacent one, as follows:

$$\Delta\text{TAT-S2}_{\text{SM-control}}(\%) = \left(\frac{\text{TAT-S2}_{\text{SM}} - \text{TAT-S2}_{\text{Control}}}{\text{TAT-S2}_{\text{Control}}} \right) \times 100$$

Positive values of $\Delta\text{TAT-S2}_{\text{SM-control}}$ mean that the time required for the S2 wavefront to depolarize the whole field of view is greater in the SM area than in the adjacent zone.

Histological analysis

Samples were fixed in 10% formaldehyde and paraffin-embedded. Pieces were cut into 4 μ m thick sections to be stained with haematoxylin–eosin and Masson's trichrome. A monoclonal antibody marker (BMDV1025, clone MY-32, IgG1-k; Accuratechemical) was used to detect skeletal fast myosin, representing mature skeletal myocytes.

Statistical analysis

Results are expressed as the mean \pm SD. The paired t-test was used to compare the incidence of VE and repeated-measures ANOVA to compare TAT, CV, and APD₉₀ in the SM and the saline groups. Pearson's correlation coefficient was used to evaluate $\Delta\text{TAT-S2}$ values and the number of injected cells. To compare the propagation patterns between SM and infarction groups, we used Fisher's exact test. A two-tailed *P*-value of <0.05 was considered significant.

Results

Histology analysis

SM-implanted samples showed whitish triangular-shape wedges embedded among the normal-coloured myocardium. The base of the wedges corresponded to the epicardium and the apex was limited to the upper mid-myocardium (Figure 1D). Lesion sizes were relatively similar. The mean epicardial area affected measured $2.4 \pm 0.4 \text{ cm}^2$, with lesions reaching a depth of $0.9 \pm 0.2 \text{ cm}$. Lesions showed the areas of vascularized fibrosis embedded within normal myocardium (Figure 1E). Connective tissue was more prominent around injection sites and included granulomas and inflammatory cells. We consistently found skeletal myocytes marked with antibodies, dispersed within preserved myocardium, and in the connective tissue (Figure 1F). Immunohistochemical staining confirmed the survival of the cells, as it marks differentiated myotubes from the original myoblasts. Skeletal myocytes were found both dispersed and arranged in small groups, adopting rounded or fusiform morphologies. The density of skeletal cells clearly declined from the areas close to the injection trajectories to the boundaries of the wedge, but differentiated skeletal cells were found slightly farther, among normal myocardium, and away from injection trajectories (Figure 1G). Saline hearts showed similar macroscopic findings with an extent and distribution of connective tissue around injection sites indistinguishable from SM hearts.

In-situ programmed electrical stimulation

No animal died spontaneously between the implant and the sacrifice surgery. No differences were found in the incidence of spontaneous VE comparing the second ($1.4 \pm 1.5 \text{ VE}$) and the third surgical procedure ($1.3 \pm 1.9 \text{ VE}$; $P = \text{NS}$) in the SM experiments. Saline experiments showed similar results (1.2 ± 1.6 vs. 1.4 ± 1.6 ; $P = \text{NS}$). Effective ventricular refractory period at 500, 400, and 300 ms were 283 ± 24 , 248 ± 18 , and $238 \pm 29 \text{ ms}$ in the SM group and 278 ± 25 , 251 ± 15 , and $234 \pm 23 \text{ ms}$ in the saline one ($P = \text{NS}$). No ventricular arrhythmia lasting more than one VE was elicited in any *in situ* heart, whether SM or saline injected. No ventricular-triggered activity, AF, or any other arrhythmias were induced in any of both groups.

Optical recordings in skeletal myoblast hearts

Isochrone maps showed homogeneous propagation patterns in both SM and adjacent zones (Figure 2A). No late depolarization zones, lines of block, or tortuous propagation patterns were found. No ventricular arrhythmia (beyond 1 VE) was induced in the isolated hearts.

Total activation time values increased after S2 beats as compared with S1 ($P = 0.001$) and as the cycle length decreased ($P = 0.0001$; Figure 3A). Although globally we did not find significant differences comparing TAT at SM versus adjacent zones ($P = 0.6$), a significant interaction was found regarding SM zone and the addition of an S2 ($P = 0.025$) indicating a slight but significantly prolonged TAT in SM zones only after an extra-stimulus. No

positive correlation was found between the extent of S2-induced propagation delay over SM zones ($\Delta\text{TAT-S2}_{\text{SM-control}}$) and the number of injected cells: $r = -0.49$ at 500 ms ($P = 0.15$) and $r = -0.61$ at 400 ms ($P = 0.06$; Figure 3D).

As the propagation patterns were homogeneous, a mean epicardial CV per isochrone map was determined. Epicardial CV was slower after S2 beats ($P = 0.012$) and decreased with the shortening of the BDCL ($P = 0.001$; Figure 3B). Although no significant differences were found between CV at SM vs. control zones ($P = 0.8$), a trend ($P = 0.2$) towards slower CV in SM zones after S2 was observed.

APD₉₀ decreased following S2 ($P = 0.002$) and with the decrease in cycle length ($P < 0.0001$; Figure 3C). However, we found no significant differences in APD₉₀ comparing SM with adjacent zones.

The experiment performed 5 months after the SM implant and the one with Cyto-D showed similar results. Propagation patterns were homogeneous and TAT, CV, and APD₉₀ determinations fell in the mean \pm SD of the remaining values.

Optical recordings in control hearts

Relatively similar results were found in the saline-injected hearts (Figure 3E–G). Total activation time analysis showed a significant interaction regarding injection zones and S2 ($P = 0.04$), suggesting a slightly prolonged TAT in the saline-injected zones only after an extra-stimulus. No significant differences were found comparing mean CV and APD₉₀. No ventricular arrhythmias were induced.

Additional experiments

The chemical infarction (Figure 2B, leftmost panels) showed late depolarization zones and lines of conduction block within a heterogeneous propagation pattern. Figure 2B also illustrates the propagation over the transition zones between normal and ischaemic-infarcted tissue (pink masks) showing overt slow conduction in infarct 1 (mean CV: 35 cm/s at S1 and 24 cm/s at S2) and 3 (36 cm/s at S1 and 28 cm/s at S2) and a heterogeneous pattern in infarct 2. Pacing with a single extra-stimulus or at 300 ms (as in SM hearts) eventually induced sustained ventricular tachycardia or ventricular fibrillation (VF) in the four isolated infarcted hearts. We classified as pathological propagation those isochrones maps showing local re-entry or overt slow conduction (CV values at 500/S2 two SD lower than the mean CV from the adjacent zones of the control hearts). All these four hearts showed pathological propagation as opposed to SM zones ($P = 0.002$).

Figure 2C shows isochrone maps of a propagated beat over the SM zone of an SM-injected heart at baseline and after adding amiodarone. Amiodarone increased TAT from 46.8 to 126 ms due to a decrease in CV from 79.3 to 25.7 cm/s. However, the homogeneous pattern of activation was preserved. Pacing at 300 ms eventually induced VF.

Discussion

This study found that SM implants induce local fibrosis but do not significantly alter epicardial wavefront propagation in the normal pig heart. The minor propagation delay found after extra-stimuli

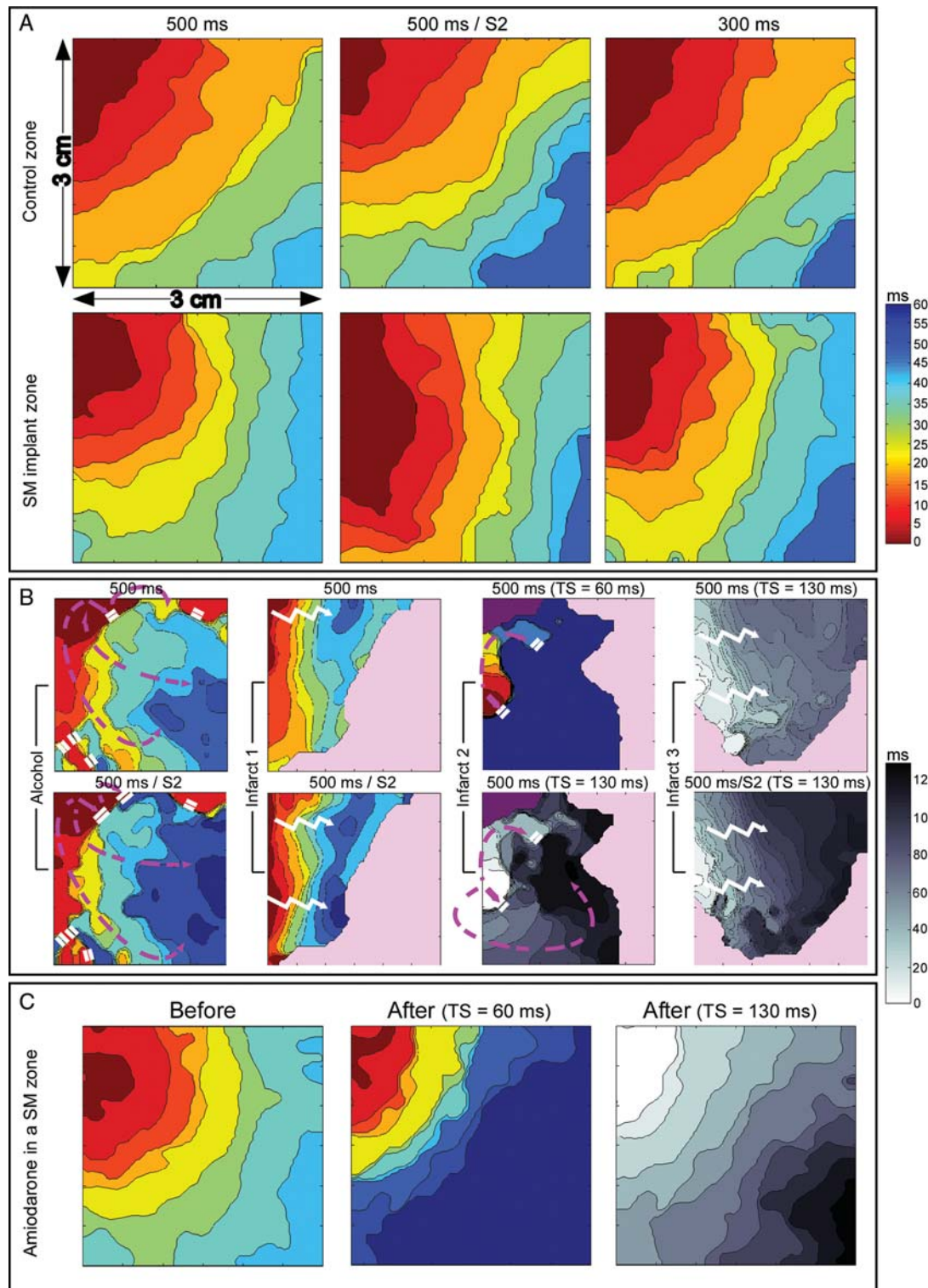


Figure 2 (A) Isochrone maps illustrating the relatively homogeneous patterns of activation of paced wavefronts in a representative heart at a control (upper row) and an adjacent SM zone (lower row). (B) Epicardial wavefront propagation over a chemically infarcted area (alcohol) and three ischaemic infarctions (1, anterior; 2 and 3, lateral). Maps reflect slow conduction, with the alcohol and infarct 2 showing significant heterogeneous propagation and conduction blocks (white parallel lines) forcing wavefronts to curve (dashed magenta arrows), paving the way for re-entry. Pink masked areas represent scar. In infarct 2, both maps show the same beat at different time scales to allow comparison with remaining maps. Purple area was excluded due to poor signal-to-noise ratio. (C) Isochrone maps of an SM-implanted area before (left) and after amiodarone (central and right maps). The rightmost panel is the same propagation map than the central one, at a time scale of 0–130 ms. Velocities significantly got slower but the propagation pattern remained homogeneous. TS, time scale.

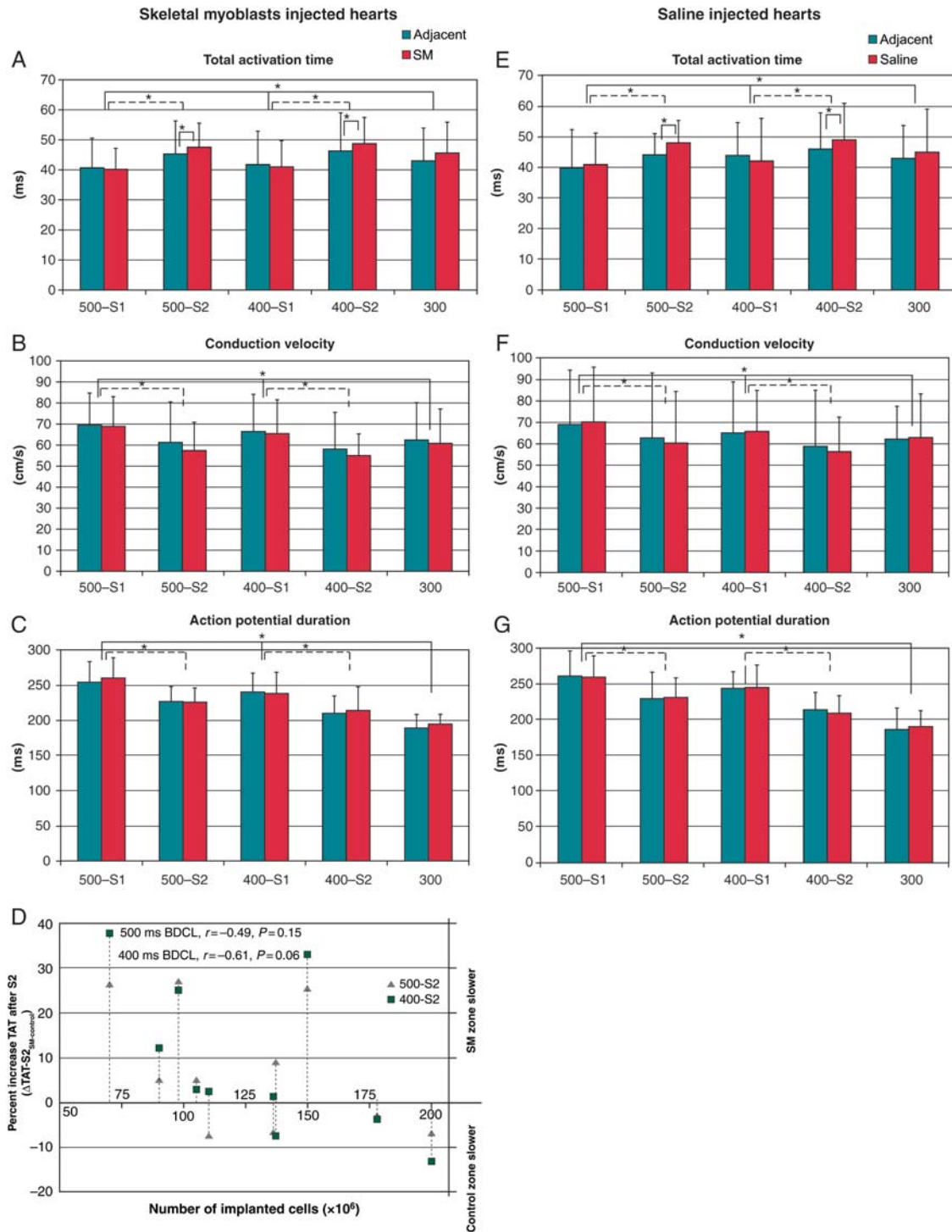


Figure 3 (A) TAT at 500, 400, and 300 ms (S1) and after adding an S2, comparing SM and adjacent control zones. TAT increased after S2 ($P = 0.001$) and as the BDCL shortened ($P = 0.0001$). Only after S2, a slight but a significant ($P = 0.025$) prolonged TAT was found in the SM zones. (B) Mean CV were slower after S2 beats ($P = 0.012$) and decreased with the BDCL shortening ($P = 0.001$). We found a minor trend ($P = 0.2$) towards slower mean CV in the SM zones after S2. (C) Repolarization times shortened following extra-stimuli ($P = 0.002$) and as the BDCL decreased ($P = 0.0001$), but there were no differences between both the zones. (D) The number of injected cells and extent of S2-induced delay over the SM zones when compared with the adjacent control areas ($\Delta\text{TAT-S2}_{\text{SM-control}}$). Values on the upper portion mean cases where the delay was higher in the SM than in the control zone. No positive correlation was found. (E–G) Similar findings in the saline group. TAT increased after S2 ($P = 0.002$), as the BDCL shortened ($P = 0.001$), and over injected zones after S2 ($P = 0.04$). CV decreased after S2 ($P = 0.01$), as the BDCL shortened ($P = 0.001$) but not significantly over injected zones. Repolarization times shortened after S2 ($P = 0.001$) and with the BDCL shortening ($P = 0.001$). * $P < 0.05$.

was not sufficient to promote proarrhythmia. Saline induced similar results, suggesting that injection-induced fibrosis and not SM cells caused this minor propagation delay.

Electrophysiological findings

Because SM do not electrically couple with surrounding myocardium, speculation has arisen suggesting that SM may act as arrhythmogenic substrates.¹⁹ We found that SM do not seem to provoke spontaneous ventricular arrhythmias, as an equivalent low rate of VE was observed before and after implantation. As the animal was under anaesthesia, we cannot rule out that catecholamines might facilitate ectopies. However, in an SM rat model, close monitoring during regular activities did not show any increase in spontaneous arrhythmias.²⁰

Pacing the whole heart *in situ* did not induce ventricular arrhythmias, suggesting that implants do not generate a clear re-entry substrate. On a more regional basis, we focused on wavefront propagation over SM and adjacent zones and found similar homogeneous patterns. No heterogeneous or slow propagation was elicited as opposed to the infarcted hearts. Even after slowing CV in an SM heart with amiodarone, no heterogeneous propagation or re-entry focus was unmasked.

We found only a slightly higher TAT over implanted areas after pacing with extra-stimuli close to refractoriness. This minor delay did not seem to be large enough to promote re-entry. This finding was found in saline-injected hearts as well, suggesting that it is probably due to induced fibrosis, more than due to dispersed non-coupled skeletal myocytes within the myocardium. The fact that increasing the number of injected cells did not increase the delay supports this hypothesis, as recently suggested by the MAGIC investigators.⁴

Arrhythmogenesis in clinical studies

Skeletal myoblast implants were associated with variable rates of ventricular arrhythmias.^{1–3,6} Reported arrhythmic events range from 0% to 20% of all implanted patients.^{2,3,6,21,22} The arrhythmic rates reported in such studies might be attributed to the patients' myocardial scars. The MAGIC trial showed that the proportion of patients who experienced ventricular arrhythmias was not significantly different between the myoblast-treated groups (which differed by the number of injected cells) and the placebo-injected group.⁴ Similar results have recently been reported in a 4-year follow-up study.⁵

Arrhythmogenesis in previous experimental models

A non-infarction model concluded that re-entrant arrhythmias can be induced in a monolayer coculture of human SM and neonatal rat ventricular myocytes.¹⁵ However, their density of SM was clearly much higher than reported engraftment rates in humans.¹⁹ In our study, SM were injected at a conventional clinical dosage. Our findings might be explained by the low density of SM achieved using the standard implantation techniques.

An infarction model in rats found that the arrhythmia inducibility was significantly higher in SM-implanted hearts.²⁰ However, these findings were not confirmed in a larger heart model (canine) in wedges of either normal or infarcted hearts.¹⁶ Probably, this may

be explained by the higher thickness of larger hearts (100 times bigger) where the trauma of injections and the whole volume of engrafted SM are proportionally smaller. In that canine model, similar transmural propagation was found in wedges with and without SM pacing from the endocardium and a slightly slower transmural propagation in SM regions pacing epicardially, with no induced transmural re-entry.

Limitations

Optical mapping was limited to the epicardium as transmural propagation has already been evaluated previously and no re-entry was elicited.¹⁶ This study was limited to normal hearts. The subtle conduction disturbances found may have a more pronounced proarrhythmic effect in a diseased environment, so we cannot speculate on any possible proarrhythmic interaction between SM implants and infarcted tissue. We believe that due to the irregular borders of ischaemic infarctions, with scars and transition zones interspersed heterogeneously, it would be extremely difficult to assess and properly quantify whether the SM implant-induced local fibrosis and the surviving cells actually modify the proarrhythmia of the ischaemic substrate. This has already been attempted¹⁶ concluding that SM implants do not modify the arrhythmic ischaemic milieu. We believe that if SM implants are clearly proarrhythmic, they should promote re-entry in the normal heart and that was not the case in our study. We mainly focused on re-entry, expanding our model to conditions known to provoke triggered activity may allow to further study such arrhythmia mechanisms.

Our stimulation protocol did not include a third extra-stimulus in order to decrease the chances of inducing probably unspecific VF episodes, being VF in the pig sometimes very difficult to defibrillate. However, two extra-stimuli protocols have previously been used with induction rates over 90% of the ones achieved using three extra-stimuli.^{23,24}

Conclusions

In the normal swine heart, myoblast implants mainly promote patches of fibrosis especially around injection trajectories, but preserving a homogeneous global conduction. Compared with adjacent zones, SM and saline implants induce a marginal prolongation of epicardial wavefront propagation times only evident after extra-stimuli. In this large mammal model, SM implants did not seem to intrinsically create significant local re-entry substrates and did not facilitate ventricular tachyarrhythmias.

Conflict of interest: none declared.

Funding

This work was supported by Fondo de Investigación Sanitaria (FIS PI 04/0747 and FIS RD06/0003/0009 Redinscor) and the Spanish Society of Cardiology (Beca Investigación Básica).

References

1. Menasche P, Hagege AA, Vilquin JT, Desnos M, Abergel E, Pouzet B *et al*. Autologous skeletal myoblast transplantation for severe postinfarction left ventricular dysfunction. *J Am Coll Cardiol* 2003;**41**:1078–83.
2. Siminiak T, Kalawski R, Fiszer D, Jerzykowska O, Rzezniczak J, Rozwadowska N *et al*. Autologous skeletal myoblast transplantation for the treatment of

- postinfarction myocardial injury: phase I clinical study with 12 months of follow-up. *Am Heart J* 2004;**148**:531–7.
3. Smits PC, van Geuns RJ, Poldermans D, Bountiokos M, Onderwater EE, Lee CH et al. Catheter-based intramyocardial injection of autologous skeletal myoblasts as a primary treatment of ischemic heart failure: clinical experience with six-month follow-up. *J Am Coll Cardiol* 2003;**42**:2063–9.
 4. Menasche P, Alfieri O, Janssens S, McKenna W, Reichenspurner H, Trinquart L et al. The Myoblast Autologous Grafting in Ischemic Cardiomyopathy (MAGIC) trial: first randomized placebo-controlled study of myoblast transplantation. *Circulation* 2008;**117**:1189–200.
 5. Veltman CE, Soliman OI, Geleijnse ML, Vletter WB, Smits PC, ten Cate FJ et al. Four-year follow-up of treatment with intramyocardial skeletal myoblasts injection in patients with ischaemic cardiomyopathy. *Eur Heart J* 2008;**29**:1386–96.
 6. Dib N, Michler RE, Pagani FD, Wright S, Kereiakes DJ, Lengerich R et al. Safety and feasibility of autologous myoblast transplantation in patients with ischemic cardiomyopathy: four-year follow-up. *Circulation* 2005;**112**:1748–55.
 7. Ben-Dor I, Fuchs S, Kornowski R. Potential hazards and technical considerations associated with myocardial cell transplantation protocols for ischemic myocardial syndrome. *J Am Coll Cardiol* 2006;**48**:1519–26.
 8. Ly HQ, Nattel S. Stem cells are not proarrhythmic: letting the genie out of the bottle. *Circulation* 2009;**119**:1824–31.
 9. Macia E, Boyden PA. Stem cell therapy is proarrhythmic. *Circulation* 2009;**119**:1814–23.
 10. Menasche P. Stem cell therapy for heart failure: are arrhythmias a real safety concern? *Circulation* 2009;**119**:2735–40.
 11. Smith RR, Barile L, Messina E, Marban E. Stem cells in the heart: what's the buzz all about? Part 2: arrhythmic risks and clinical studies. *Heart Rhythm* 2008;**5**:880–7.
 12. Al AN, Carrion C, Ghostine S, Garcin I, Vilquin JT, Hagege AA et al. Long-term (1 year) functional and histological results of autologous skeletal muscle cells transplantation in rat. *Cardiovasc Res* 2003;**58**:142–8.
 13. Taylor DA, Atkins BZ, Hungspreugs P, Jones TR, Reedy MC, Hutcheson KA et al. Regenerating functional myocardium: improved performance after skeletal myoblast transplantation. *Nat Med* 1998;**4**:929–33.
 14. Leobon B, Garcin I, Menasche P, Vilquin JT, Audinat E, Charpak S. Myoblasts transplanted into rat infarcted myocardium are functionally isolated from their host. *Proc Natl Acad Sci USA* 2003;**100**:7808–11.
 15. Abraham MR, Henrikson CA, Tung L, Chang MG, Aon M, Xue T et al. Anti-arrhythmic engineering of skeletal myoblasts for cardiac transplantation. *Circ Res* 2005;**97**:159–67.
 16. Fouts K, Fernandes B, Mal N, Liu J, Laurita KR. Electrophysiological consequence of skeletal myoblast transplantation in normal and infarcted canine myocardium. *Heart Rhythm* 2006;**3**:452–61.
 17. Moreno J, Zaitsev AV, Warren M, Berenfeld O, Kalifa J, Lucca E et al. Effect of remodelling, stretch and ischaemia on ventricular fibrillation frequency and dynamics in a heart failure model. *Cardiovasc Res* 2005;**65**:158–66.
 18. Bayly PV, KenKnight BH, Rogers JM, Hillsley RE, Ideker RE, Smith WM. Estimation of conduction velocity vector fields from epicardial mapping data. *IEEE Trans Biomed Eng* 1998;**45**:563–71.
 19. Pagani FD, DerSimonian H, Zawadzka A, Wetzel K, Edge AS, Jacoby DB et al. Autologous skeletal myoblasts transplanted to ischemia-damaged myocardium in humans. Histological analysis of cell survival and differentiation. *J Am Coll Cardiol* 2003;**41**:879–88.
 20. Fernandes S, Amirault JC, Lande G, Nguyen JM, Forest V, Bignolais O et al. Autologous myoblast transplantation after myocardial infarction increases the inducibility of ventricular arrhythmias. *Cardiovasc Res* 2006;**69**:348–58.
 21. Gavira JJ, Herreros J, Perez A, Garcia-Velloso MJ, Barba J, Martin-Herrero F et al. Autologous skeletal myoblast transplantation in patients with nonacute myocardial infarction: 1-year follow-up. *J Thorac Cardiovasc Surg* 2006;**131**:799–804.
 22. Siminiak T, Fiszer D, Jerzykowska O, Grygielska B, Rozwadowska N, Kalmucki P et al. Percutaneous trans-coronary-venous transplantation of autologous skeletal myoblasts in the treatment of post-infarction myocardial contractility impairment: the POZNAN trial. *Eur Heart J* 2005;**26**:1188–95.
 23. Groban L, Deal DD, Vernon JC, James RL, Butterworth J. Ventricular arrhythmias with or without programmed electrical stimulation after incremental overdosage with lidocaine, bupivacaine, levobupivacaine, and ropivacaine. *Anesth Analg* 2000;**91**:1103–11.
 24. Simonson JS, Gang ES, Mandel W, Peter T. Increasing the yield of ventricular tachycardia induction: a prospective, randomized comparative study of the standard ventricular stimulation protocol to a short-to-long protocol and a new two-site protocol. *Am Heart J* 1991;**121**:68–76.